SMALL-FIELD ANGIOGRAPHIC IMAGING OF TUMOR BLOOD VESSELS USING SYNCHROTRON RADIATION

K. Umetani[1], T. Yamashita[2], N. Maehara[2], S. Imai[2], Y. Kajihara[2]
[1] Life & Environment Division, Japan Synchrotron Radiation Research Institute, SPring-8, Hyogo, Japan
[2] Department of Diagnostic Radiology, Kawasaki Medical School, Okayama, Japan

Abstract-**Microangiography with about 10 μm resolution has been carried out for depicting angiogenic vessels in a rabbit model of cancer using a high-resolution detector and a third generation synchrotron radiation source at SPring-8. In synchrotron radiation radiography, a long source-to-object distance and a small source spot can produce high-resolution images. VX2 carcinoma had been transplanted in a rabbit auricle. By using this imaging system, small tumor blood vessels with diameters of 20-30 μm in an immature vascular network produced by angiogenesis were visualized after contrast material injection to the auricular artery.**

I. INTRODUCTION

Diagnostic imaging using synchrotron radiation has been investigated since Rubenstein and his coworkers reported dual-energy iodine-K-edge subtraction coronary angiography for a relatively safe intravenous angiography technique in 1981 [1]. The difference in X-ray absorption by iodine contrast material at energies just above and just below the iodine K-edge energy has been used for high-sensitivity imaging of diluted contrast material. Research groups at several synchrotron radiation facilities have improved the dual-energy imaging systems for human studies [2-4]. In Japan the first human study of intravenous coronary angiography was performed using a single-energy approach in May 1996 [5]. In the single-energy approach, the monochromatized X-ray at energies just above the iodine K-edge energy was used to produce the highest contrast image of iodine contrast material. The single-energy approach was also applied to intra-arterial microangiography [6]. The microangiography system was investigated as a diagnostic tool for circulatory disorders and early stage malignant tumors [7,8]. At SPring-8, a digital microangiography system with about 10 μm resolution was developed using a detector designed for X-ray direct detection [9]. Images of tumor blood vessels induced by transplanted VX2 carcinomas in rabbit auricles were obtained after the iodine contrast agent injection to the auricular artery. Tumor-induced small blood vessels with diameters of 20-30 μm were visualized at the monochromatized X-ray energy of 33.2 keV just above the iodine K-edge energy.

II. METHODOLOGY

A. Sharpness

Radiographic unsharpness results from geometric and detector unsharpness. Geometric unsharpness is affected by the size of the X-ray source in combination with source-to-object and object-to-detector distances. In conventional medical X-ray imaging using an X-ray tube, the highest spatial resolution is around 30 μm. However, it is attained by a mammography unit that produces a single high-resolution radiograph using an intensifying screen and film combination [10].

In the real-time imaging, a conventional angiography system is not oriented to the detection of small vessels having diameters of 200 μm or less because the spatial resolution is restricted by the use of an X-ray image intensifier. It is used mainly for large-field angiographic imaging with a 1024× 1024-pixel digital format.

On the other hand, microangiography with a resolution higher than 30 μm has been carried out using a high-resolution detector and a nearly parallel X-ray beam provided by a third generation synchrotron radiation source at SPring-8. In synchrotron radiation radiography, the long source-to-object distance and the small source size can overcome geometric unsharpness.

B. Synchrotron radiation

A photon beam generated by bending the path of electrons at relativistic speeds is called synchrotron radiation. Coronary angiography studies using the monochromatized X-ray have been performed mainly at a second generation of synchrotron radiation facilities. A first generation of synchrotrons was used primarily for particle physics and any research done with synchrotron radiation was parasitic. Synchrotron radiation was an undesired energy-loss mechanism for the first generation of synchrotrons. The second generation of synchrotrons is dedicated to the production of synchrotron radiation providing a steady source of X-ray for research.

The third generation of synchrotron radiation is characterized by small electron-beam size that is a small source spot and by radiation beams of very high spectral brightness. There are only three hard X-ray third-generation of synchrotron radiation facilities. The SPring-8 [11] opened in 1997 and joins the European Synchrotron Radiation Facility (ESRF) in Grenoble, which opened in 1994 [12], and the Advanced Photon Source (APS) at the Argonne National Laboratory in Illinois, which opened in 1996 [13].

In the storage ring, the high-energy electron beam travels in a curved trajectory controlled by bending magnets and focusing magnets. The electron beam travels alternately straight sections and arc-shaped bending-magnet sections. By bending the path of electrons at relativistic speeds, X-rays are

0-7803-7211-5/01$10.00©2001 IEEE

Report Documentation Page

Report Date	Report Type	Dates Covered (from... to)
25 Oct 2001	N/A	-

Title and Subtitle Small-Field Angiographic Imaging of Tumor Blood Vessels Using Synchrotron Radiation	**Contract Number**
	Grant Number
	Program Element Number
Author(s)	**Project Number**
	Task Number
	Work Unit Number
Performing Organization Name(s) and Address(es) Life & Environment Division Japan Synchrotron Radiation Research Institute SPring-8 Hyogo, Japan	**Performing Organization Report Number**
Sponsoring/Monitoring Agency Name(s) and Address(es) US Army Research Development & Standardization Group (UK) PSC 802 Box 15 FPO AE 09499-1500	**Sponsor/Monitor's Acronym(s)**
	Sponsor/Monitor's Report Number(s)

Distribution/Availability Statement
Approved for public release, distribution unlimited

Supplementary Notes
Papers from 23rd Annual International Conference of the IEEE Engineering in Medicine and Biology Society, October 25-28, 2001, held in Istanbul, Turkey. See also ADM001351 for entire conference on cd-rom.

Abstract

Subject Terms

Report Classification unclassified	**Classification of this page** unclassified
Classification of Abstract unclassified	**Limitation of Abstract** UU

Number of Pages
4

emitted at each bending magnet in a direction tangential to the electron beam trajectory. Synchrotron radiation produced by bending magnets is a fan-shaped beam that is horizontally wide and vertically narrow.

The medium length bending-magnet beamline BL20B2 at SPring-8 is dedicated mainly to basic medical science using biological specimens and small animals [9]. The construction of the beamline was completed in June 1999. BL20B2 has been operational for users since October 1999. The full length of the beamline is 215 meters from the X-ray source to the end station. The X-ray beam produced by the bending magnet passes out of the experimental hall surrounding the storage ring and enters a satellite laboratory, the Biomedical Imaging Center. A fan-shaped beam with a cross-section size of 75 mm width by 5 mm height is produced in the experimental hall. A 300×20 mm beam is obtained 200 meters from the source in the Biomedical Imaging Center.

C. High-resolution detector

The direct-sensing detector consists of an X-ray direct-sensing pickup tube with a beryllium faceplate for X-ray incidence to the photoconductive layer. Absorbed X-rays in the photoconductive layer are directly converted to photoelectrons and signal charges are readout by electron beam scanning.

An X-ray direct-sensing vidicon-type pickup-tube camera was developed in the 1960's with a PbO photoconductive layer for the observation of real-time topography images combined with a high power X-ray generator. The resolution of the direct-sensing pickup tube had been improved. The X-ray SATICON tube with an amorphous photoconductive Se-As alloy target was developed for the use of synchrotron radiation experiments of live topography at the Photon Factory [14].

The direct-sensing camera was further improved with the introduction of high-definition television (HDTV) which increases resolution to 1050 scanning lines. The new X-ray SATICON camera has the same resolution of 1050 scanning lines. The new camera, however, can take images at the maximum speed of 30 images/s. The digital images are acquired by a digital-image acquisition system after analog-to-digital conversion synchronizing the timing with the electron beam scanning in the pickup tube. High-resolution images are stored in digital frame memory with the 10-bit resolution.

D. Imaging system

Experimental set-up for the microangiographic imaging at the BL20B2 beamline is shown in Fig. 1. Synchrotron radiation produced by the bending magnet is monochromatized by a silicon double-crystal monochromator. The monochromatized X-ray comes out from a vacuum tube into the atmosphere by passing through a beryllium window. The X-rays transmitted through the object were detected by the imaging detector.

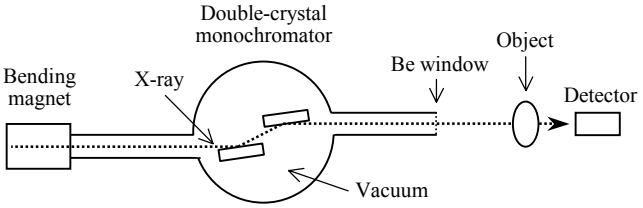

Fig. 1. Schematic diagram of experimental setup for microangiographic imaging using monochromatized synchrotron radiation.

Experiments were performed in the Biomedical Imaging Center. The distance between the source point in the bending magnet and the detector was 210 meters. The nearly parallel X-ray beam was used for imaging without geometrical unsharpnes in the Biomedical Imaging Center because of the small size of the X-ray source and the very long source-to-object distance.

The storage ring was operated at 8 GeV electron beam energy and the beam current was 80-100 mA. The energy of monochromatized X-ray was adjusted to 33.2 keV just above the iodine K-edge energy to produce the highest contrast image of iodine contrast material. X-ray flux at the object position was about 10^7 photons/mm^2/s.

III. RESULTS

A. Resolution

The performance of the direct-sensing pickup-tube camera was evaluated by taking an image of a spatial resolution chart. Images were obtained in the 1050 scanning-line mode of the camera at an input field size of 9.5×9.5 mm. The digital images were acquired after analog-to-digital conversion synchronizing the timing with the electron beam scanning in the pickup tube. High-resolution images were stored in digital frame memory with the 10-bit resolution and 1024×1024-pixel digital format. The maximum speed of imaging was 30 images/s.

In the bar pattern chart image, the stripes of 12 μm width appeared but the 9 μm stripes did not appeared [15]. The limiting spatial resolution is around 10 μm that is equal to the equivalent pixel size projected onto the photoconductive layer. By using this detector, small blood vessels with diameters of 20-30 μm can be visualized.

B. Angiographic imaging

A tumor stimulates the growth of small blood vessels for feeding the tumor itself. It has been proposed that tumor-induced small vessels are an intrinsic part of tumor development and progression. The growth rate of tumors is slow before the blood vessel formation and rapid after the vessel formation [16-18].

Radiographic depiction of tumor-induced small vessels that feed a space-occupying lesion is useful tool for the

diagnosis of malignant tumors. However, a conventional angiography system used in a hospital has considerable limitations in providing images of small blood vessels with diameters of less than 200 μm.

The purpose of the present study was to evaluate the depiction of small vessels in the immature vascular network produced by angiogenesis in a rabbit auricle, into which VX2 carcinoma had been transplanted. Japanese white rabbits weighing about 3.0 kg were used for imaging. The rabbits were anesthetized with an intravenous injection of pentobarbital sodium. The VX2 cancer cells were subcutaneously injected into the auricles.

Microangiography was performed at one, three, and seven days after transplantation. The rabbits were similarly anesthetized. A 24 gauge intracatheter was inserted into the auricular artery. The contrast material used for imaging was 2.4 ml per one injection at a speed of 0.2 ml/s. The contrast agent was injected into the auricular artery by an auto injector that was controlled by the digital-image acquisition system.

Microangiographic images were obtained continuously at a speed of 5 images/s after the contrast agent injection. The exposure time per image was 0.2 s. Images were stored in digital frame memory with the 10-bit resolution and 1024× 1024-pixel digital format controlled by the digital-image acquisition system. 70-100 images were stored in total. All of our experiments on animals conformed to the SPring-8 Guide for the Care and Use of Laboratory Animals.

Representative angiographic images of the transplanted tumors taken at seven days after transplantation by synchrotron radiation microangiography are shown in Fig. 2. A time interval of each image is 0.8 s. The first and second images show the network of tumor-feeding arteries originating from the first-order branch of the proximal auricular artery. Small blood vessels of 20-30 μm in diameter were observed in the second image. The third and fourth images show the tumor encircled with the network of veins. In the fourth image, the white dotted circle shows the size of the tumor.

IV. Discussion

The microangiography system using monochromatized synchrotron radiation and the high-resolution direct-sensing detector can visualize immature vascular networks in transplanted malignant tumors, and is useful for the depiction and quantification of angiogenic vessels in the rabbit model of cancer. The immature vascular networks could not be demonstrated by conventional angiography.

The angiographic system has advantages over conventional system. Monochromatized X-ray produces the highest contrast image of iodine contrast material at the energy of 33.2 keV just above the iodine K-edge energy, and allows detection of small amounts of iodine contrast agent in small vessels.

Radiographic unsharpness results from geometric and detector unsharpness. Synchrotron radiation is a nearly parallel X-ray beam provided by the third generation synchrotron radiation source at SPring-8. The geometry of

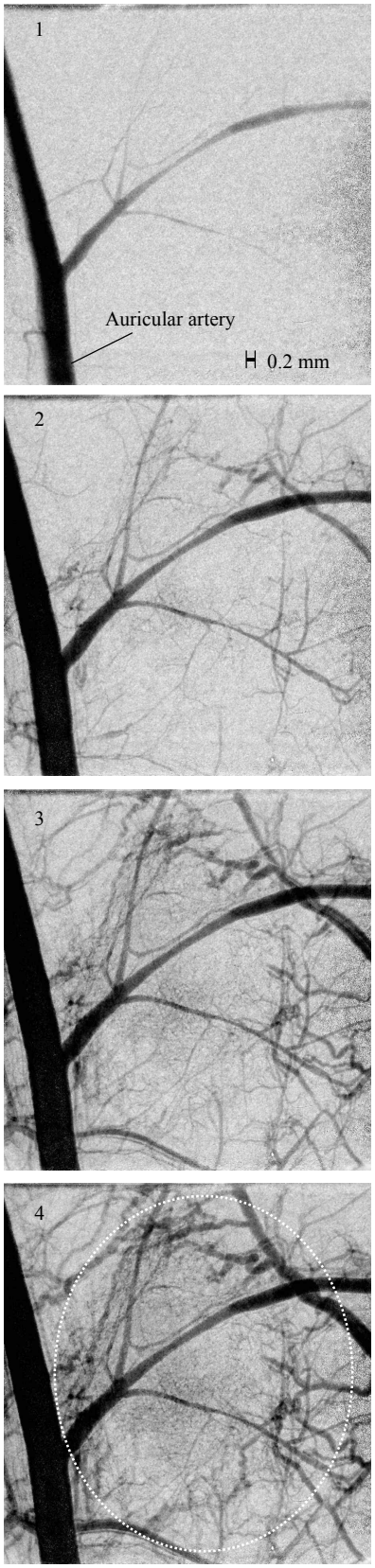

Fig. 2. Microangiographic images of tumor blood vessels induced by VX2 carcinoma at seven days after transplantation in rabbit auricle.

long source-to-object distance can overcome geometric unsharpness.

Imaging detectors used for conventional angiography systems are not oriented to the detection of small vessels because of large-field angiographic imaging with the 1024× 1024-pixel digital format. Our small-field direct-sensing detector, however, achieved the limiting spatial resolution of around 10 μm.

V. Conclusion

The synchrotron radiation microangiography system allows depiction of tumor-induced small blood vessels with diameters of 20-30 μm. This system can demonstrate immature vascular networks in transplanted malignant tumors in the rabbit auricle. The synchrotron radiation system will be a useful tool for evaluating the microangioarchitecture of malignant tumors.

Acknowledgment

The authors would like to thank Tadaaki Hirai, Toshiaki Kawai, and Katsuhiko Suzuki of Hamamatsu Photonics K.K. for development of the X-ray SATICON tubes. The authors also thank Sadao Takahashi of Hitachi Denshi Techno-System, Ltd. for providing the camera system used for the imaging experiment. The authors wish to acknowledge the contributions of Dr. Naoto Yagi and Dr. Katsuhito Yamasaki at SPring-8.

References

[1] E. Rubenstein, E. B. Hughes, L. E. Campbell, R. Hofstadter, R. L. Kirk, T. J. Krolicki, J. P. Stone, S. Wilson, H. D. Zeman, W. R. Brody, A. Macovski, and A. C. Thompson, "Synchrotron radiation and its application to digital subtraction angiography," *Proc. SPIE*, Vol. 314, pp. 42-49, January 1981.

[2] E. Rubenstein, G. S. Brown, D. Chapman, R. F. Garrett, J. C. Giacomini, N. Gmur, H. J. Gordon, W. M. Lavender, J. Morrison, W. Thomlinson, A. C. Thompson, and H. Zeman, "Synchrotron radiation coronary angiography in humans," in *Synchrotron Radiation in the Biosciences*, B. Chance *et al.*, Eds. New York: Oxford University Press, 1994, pp. 639-645.

[3] T. Dill, W. -R. Dix, C. W. Hamm, M. Jung, W. Kupper, M. Lohmann, B. Reime, and R. Ventura, "Intravenous coronary angiography: experience in 276 patients," *Synchrotron Radiation News*, Vol. 11, pp. 12-20, March/April 1998.

[4] H. Elleaume, S. Fiedler, F. Estève, B. Bertrand, A.M. Charvet, A. Bravin, P. Berkvens, G. Berruyer, T. Brochard, Y. Dabin, A. Draperi, G. Goujon, G. Le Duc, C. Nemoz, M. Perez, M. Renier, P. Suortti, W. Thomlinson, and J.F. Le Bas, "First Human Coronary Angiography at the ESRF," *ESRF Highlights 2000*, pp. 11-12, February 2001.

[5] S. Ohtsuka, Y. Sugishita, T. Takeda, Y. Itai, J. Tada, K. Hyodo, and M. Ando, "Dynamic intravenous coronary angiography using 2D monochromatic synchrotron radiation," *Br. J. Radiol.*, Vol. 72, pp. 24-28, January 1999.

[6] K. Umetani, H. Ueki, T. Takeda, Y. Itai, H. Mori, E. Tanaka, M. Uddin-Mohammed, Y. Shinozaki, M. Akisada, and Y. Sasaki, "High-spatial-resolution and real-time medical imaging using a high-sensitivity HARPICON camera," *J. Synchrotron Rad.*, Vol. 5, pp. 1130-1132, May 1998.

[7] H. Mori, K. Hyodo, E. Tanaka, M. Uddin-Mohammed, A. Yamakawa, Y. Shinozaki, H. Nakazawa, Y. Tanaka, T. Sekka, Y. Iwata, S. Handa, K. Umetani, H. Ueki, T. Yokoyama, K. Tanioka, M. Kubota, H. Hosaka, N. Ishikawa, and M. Ando, "Small-vessel radiography in situ with monochromatic synchrotron radiation," *Radiology*, Vol. 201, pp. 173-177, October 1996.

[8] S. Takeshita, T. Isshiki, H. Mori, E. Tanaka, K. Eto, Y. Miyazawa, A. Tanaka, Y. Shinozaki, K. Hyodo, M. Ando, M. Kubota, K. Tanioka, K. Umetani, M. Ochiai, T. Sato, and H. Miyashita, "Use of synchrotron radiation microangiography to assess development of small collateral arteries in a rat model of hindlimb ischemia," *Circulation*, Vol. 95, pp. 805-808, February 1997.

[9] K. Umetani, N. Yagi, Y. Suzuki, Y. Ogasawara, F. Kajiya, T. Matsumoto, H. Tachibana, M. Goto, T. Yamashita, S. Imai, and Y. Kajihara, "Observation and analysis of microcirculation using high-spatial-resolution image detectors and synchrotron radiation," *Proc. SPIE*, Vol. 3977, pp. 522-533, April 2000.

[10] M. M. Goodsitt, H. -P. Chan, and B. Liu, "Investigation of the line-pair pattern method for evaluating mammographic focal spot performance," *Med. Phys.*, Vol. 24, pp. 11-15, January 1997.

[11] H. Kamitsubo, "SPring-8 program," *J. Synchrotron Rad.*, Vol. 5, pp. 162-167, May 1998.

[12] J. M. Filhol, and L. Hardy, "Status report of the ESRF," in *Proc. 1997 Particle Accelerator Conference*, M. Comyn *et al.*, eds. New Jersey: the Institute of Electronical and Electronics Engineers, Inc., 1998, pp. 751-753.

[13] D. E. Moncton, "The Advanced Photon Source: performance and results from early operation," *J. Synchrotron Rad.*, Vol. 5, pp.155-157, May 1998.

[14] J. Chikawa, F. Sato, T. Kawamura, T. Kuriyama, T. Yamashita, and N. Goto, "A high-resolution video camera tube for live X-ray topography using synchrotron radiation," in *X-ray Instrumentation for the Photon Factory: Dynamic Analysis of Micro Structures in Matter*, S. Hosoya *et al.*, eds. Tokyo : KTK Scientific Publishers, 1986, pp145-157.

[15] K. Umetani, T. Hirai, and S. Takahashi, "Medical imaging detectors for real-time micro-radiography," *SPring-8 Annual Report 1999*, pp. 144-145, December 2000.

[16] J. Folkman, "Tumor angiogenesis," Adv. Cancer Res., Vol. 43, pp. 175-203, 1985.

[17] J. Folkman, "What is the evidence that tumors are angiogenesis dependent ?," *J. Natl. Cancer Inst.*, Vol. 82, pp. 4-6, January 1990 .

[18] J. Folkman, "Angiogenesis in cancer, vascular, rheumatoid and other disease," *Nat. Med.*, Vol. 1, pp. 27-31, January 1995.